ChemPubSoc Europe

DOI: 10.1002/cmdc.201800641

CHEMMEDCHEM Full Papers

Synthesis, Biological Evaluation, and Molecular Docking of Combretastatin and Colchicine Derivatives and their hCE1-Activated Prodrugs as Antiviral Agents

Michael Richter,[a] Veaceslav Boldescu,[a, d] Dominik Graf,[a] Felix Streicher,[a] Anatoli Dimoglo,[b] Ralf Bartenschlager,[c] and Christian D. Klein*[a]

Recent studies indicate that tubulin can be a host factor for vector-borne flaviviruses like dengue (DENV) and Zika (ZIKV), and inhibitors of tubulin polymerization such as colchicine have been demonstrated to decrease virus replication. However, toxicity limits the application of these compounds. Herein we report prodrugs based on combretastatin and colchicine derivatives that contain an ester cleavage site for human carboxylesterase, a highly abundant enzyme in monocytes and hepatocytes targeted by DENV. Relative to their parent compounds, the cytotoxicity of these prodrugs was reduced by several orders of magnitude. All synthesized prodrugs containing a leucine ester were hydrolyzed by the esterase in vitro. In contrast to previous reports, the phenylglycine esters were not cleaved by human carboxylesterase. The antiviral activity of combretastatin, colchicine, and selected prodrugs against DENV and ZIKV in cell culture was observed at low micromolar and sub-micromolar concentrations. In addition, docking studies were performed to understand the binding mode of the studied compounds to tubulin.

Introduction

The development of new antiviral agents against flaviviruses remains a great necessity due to the lack of efficient vaccines or other options for prevention or treatment of infectious diseases caused by some of the most widespread species of the *Flaviviridae* family: dengue, West Nile, and Zika viruses. Dengue is considered the most common viral infection transmitted by an arthropod, with an estimated number of infections ranging from 50 to 100 million per year, of which 10–20 thousand are lethal.[1,2] The increasing number of co-circulating flaviviruses, as well as the emergence of new human infections caused by arboviruses,[3] make it desirable to develop agents with broad-spectrum activity.[4] It appears promising to target host factors; this strategy carries a lower risk of resistance development and has a higher potential for broad-spectrum activity.[5] A major disadvantage and risk of targeting host factors, however, can arise from interference with physiological host processes and subsequent toxicity. One possible way to overcome this disadvantage is the design of prodrugs that are specifically activated within virus-infected cells, or within those cells that are preferably targeted by the virus.

The present work is based on the hypothesis that agents influencing microtubule dynamics could be used in sub-cytotoxic concentrations as systemic antiviral agents. A related successful example from clinical practice is the use of podophyllotoxin as topical medication (Podofilox) to treat warts that are often induced by infections with the human papilloma virus.[6]

Tubulin ligands have the potential to inhibit the replication of those viruses that depend on the microtubule network, such as ZIKV and DENV.[7] Thus, these inhibitors might be suitable as possible broad-spectrum anti-flaviviral or even broad-spectrum antiviral agents.

We hypothesized that prodrugs of tubulin polymerization inhibitors (TPIs) which are specifically activated in cells of the monocyte–macrophage lineage and hepatocytes, which are preferential targets of flaviviruses, would spare unaffected cells and tissues from the nonspecific and toxic effects of tubulin inhibition.

Microtubules and the cytoskeleton have been intensively studied and found to be involved in several steps of the flaviviral replication cycle, such as viral entry, intracellular transport, virion assembly, and egress.[8,9] Although the involvement of microtubules in cell entry of DENV has been reported to be crucial,[10,11] other reports suggest a microtubule-independent cell entry of different DENV serotypes.[12] Also in these cases, microtubules might be a nonessential, but nevertheless supportive factor for the infection of cells.[12]

[a] M. Richter, Dr. V. Boldescu, Dr. D. Graf, F. Streicher, Prof. Dr. C. D. Klein
Institute of Pharmacy and Molecular Biotechnology, Heidelberg University, INF 364, 69120 Heidelberg (Germany)
E-mail: c.klein@uni-heidelberg.de

[b] Prof. A. Dimoglo
Faculty of Engineering, Düzce University, Düzce (Turkey)

[c] Prof. Dr. R. Bartenschlager
Department of Infectious Diseases, Molecular Virology, Heidelberg University, INF 344, 69120 Heidelberg (Germany), and German Center for Infection Research, Heidelberg Partner Site

[d] Dr. V. Boldescu
Institute of Chemistry, Laboratory of Organic Synthesis and Biopharmaceuticals, Moldova Academy of Sciences, Academiei str. 3, MD2028 Chisinau (Moldova)

The ORCID identification number(s) for the author(s) of this article can be found under: https://doi.org/10.1002/cmdc.201800641.

The intracellular transport of viral particles in the host cell, including their trafficking to assembly sites in later stages of the infection, is performed by microtubules and their associated proteins.[13] Tubulin was found to be 3.3-fold overexpressed in patients with dengue hemorrhagic fever.[14] Acosta et al. have demonstrated that inhibitors of microtubule polymerization cause a significant decrease in virus production.[15] These authors also suggested that the structural integrity of the microtubule network is required for efficient entry of DENV into cells.

Tubulin structures in DENV-infected cells were described to assist in the scaffold assembly of the virus through interactions with the viral envelope (E) protein.[16] The microtubule-stabilizing agent paclitaxel has been shown to decrease the viral titer of ZIKV in Huh7 cells, which suggests an important role of microtubule dynamics in ZIKV replication.[7] Chen et al. have suggested that a microtubule destabilizing agent, colchicine, induced an enhanced release of DENV from infected cells,[12] however the influence on viral replication has not been explored in that study.

The main target cells for DENV are immune cells of the macrophage-monocytic lineage (Langerhans cells, splenic macrophages, tissue macrophages, Kupffer cells) as well as hepatocytes and endothelial cells.[17,18] A potential activator enzyme for prodrugs that is highly expressed in these cells is the human carboxylesterase-1 (hCE1).[19,20] Depending on the design of the prodrug, intracellular hydrolysis of a drug-ester conjugate by hCE1 results in the formation of an active compound with increased polarity, lower membrane permeability and a tendency to accumulate within the targeted cells.[21] The concept has already been applied to some antiarthritic[21] compounds and imaging agents.[22] hCE1 was described to cleave preferably at the two cleavage motifs shown in Figure 1, the cyclopentanol esters of phenylglycine (Phg) and leucine. We therefore chose to use these motifs in the design of hCE1-activated tubulin-ligand prodrugs.

Numerous microtubule-stabilizing and -destabilizing compounds are derived from natural products and have been modified by partial or complete synthesis. The microtubule-destabilizing alkaloid colchicine binds into a pocket between the α- and β-tubulin subunits[23] and thereby inhibits tubulin polymerization. The "colchicine-binding site" is also targeted by the combretastatins, another group of natural products[24] whose most potent member (combretastatin A-4) has similar affinity for tubulin as colchicine.[25] The combretastatins and their synthetic analogues are accessible via Wittig reaction of two substituted aromatic rings, which allows a straightforward synthesis of many derivatives. Moreover, functional groups like amines and carboxylic acids can be attached, rendering combretastatin an attractive object for derivatization. As shown in Figure 2, the hydroxy group at position 3 of the B-ring is not essential for activity, which makes this position attractive for the attachment of prodrug moieties. A phosphoric acid ester attached at this position yields a prodrug with increased aqueous solubility (fosbretabulin) which showed potent antitumor activity in phase II clinical trials.[26]

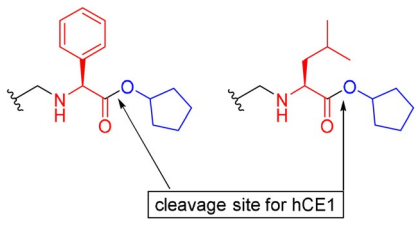

Figure 1. hCE1-selective motifs according to Needham et al.[21]: Cyclopentyl esters of phenylglycine and leucine are hydrolyzed by human carboxylesterase 1 to form cyclopentanol and the corresponding carboxylate.

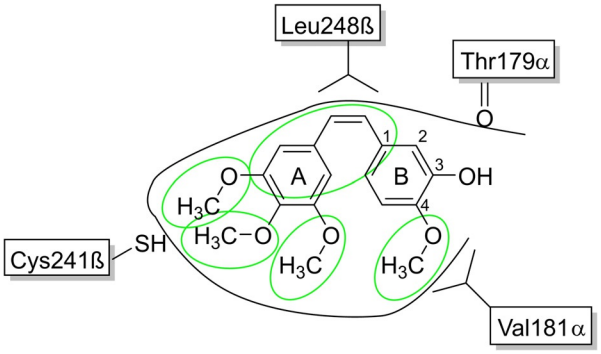

Figure 2. Structure-activity relationships of the combretastatins. Shown is combretastatin A-4 in the tubulin binding pocket (PDB ID: 5LYJ) with the established labelling of the carbon atoms. Essential structural elements are marked in green: in particular, these are the four methoxy groups and the *cis*-configured double bond with the surrounding hydrophobic area.[24] For reviews of the SAR, see refs. [27–29].

The main problem regarding the use of colchicine and other tubulin polymerization destabilizers as antiviral drugs is their high systemic toxicity. Colchicine causes a complete inhibition of tubulin assembly at sub-stoichiometric concentrations[31] and has strong anti-angiogenic effects, a typical feature of microtubule disrupting agents, which is now seen to provide a promising approach for the treatment of cancer.[32,33]

Previous attempts to decrease the systemic toxicity of colchicine often resulted in a significant drop or total loss of biological activity.[34] A structural analysis of the colchicine-binding site of tubulin reveals that mainly the A-ring of colchicine and its substituents interact with the target, whereas the B- and especially C-ring offer potential for derivatization for the purpose of decreasing toxicity (Figure 3).

Although sterically limited due to the structure of the colchicine-binding site, the most prominent position for introducing structural alterations is the 10-methoxy group situated in ring C. Replacements at this position and the amino group at position 7 resulted in compounds with similar or lower cytotoxicity as that of colchicine and higher selectivity of action toward specific cells, such as cancer cells.[33,35–37] Particularly promising is the replacement of the 10-methoxy group by amine-containing scaffolds such as amino acids, or ammonia.[38,39] Small substituents in that position are well tolerated, whereas long or bulky moieties have a detrimental effect on activity.[33]

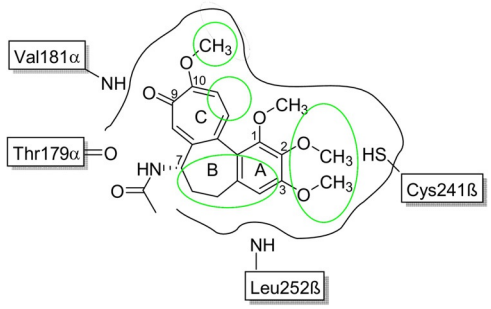

Figure 3. Outline of the most important characteristics of a molecule of colchicine situated in a colchicine-binding site of tubulin (PDB ID: 4O2B) as identified by SAR, hydropathic analysis, and 3D-QSAR. The area marked with green indicates specific steric barriers of the binding site.[30]

Considering the SAR outlined above, the tolerance of tubulin toward modified ligands, and the synthetic accessibilities, we chose position B-3 in combretastatin (see Figure 2) and position 10 in colchicine (see Figure 3) as connecting points for attachment of prodrug moieties. We anticipated that larger moieties, i.e., those present in the prodrugs in these positions, would cause a loss in tubulin affinity, rendering the prodrugs inactive. In contrast, upon cleavage of the prodrug, we expected the remaining attachment structures to be tolerated by tubulin.

Molecular modelling of biochemical processes makes it possible to understand at a deeper level the mechanism of interaction in the ligand–protein complex.[40] This knowledge can be used to search for and synthesize new active compounds with specific properties. Based on available experimental data about the inhibition of tubulin polymerization, in recent years there have been many studies related to the molecular modelling and docking of various classes of chemical compounds in the colchicine-binding site of tubulin.[41–49]

In one of the first studies[41,42] devoted to the docking of various ligands into the colchicine-binding site of tubulin, it has been shown that the binding of colchicine derivatives to the active site of α-tubulin is due to the formation of hydrogen bonds of colchicines with residues such as His28, Ser232, Cys356, and Arg320. For β-tubulin, binding occurs with Thr33 and Tyr36.

In several subsequent studies,[43–45] cytotoxic properties of the compounds turned out to be due to their ability to inhibit the polymerization of tubulin. Based on the results of docking, the authors draw conclusions about the relationship between compound cytotoxicity and the way the compounds dock onto the receptor. This correlates well with the antitumor activity of these compounds. Other studies[46,48–51] have been devoted to the modelling of pharmacophores, docking and virtual screening of various tubulin inhibitors. The authors use the obtained pharmacophore model of inhibition of tubulin to draw conclusions on the antitumor activity relative to new potentially active compounds.

Results and Discussion

Synthesis of combretastatin- and colchicine-based derivatives

The hCE1-sensitive motifs used for derivatization were obtained according to the method described by Charlton et al.[22] with modification for the phenylglycine-based motif as described in the Experimental Section. The obtained motifs were connected to the active compounds via an amide bond. Therefore, in the structure of combretastatin, the hydroxy group was replaced by a carboxylic acid group. To modulate activity, toxicity and lipophilicity of the esters, alkyl spacers based on 4-aminobutyric acid and 8-aminooctanoic acid were inserted between combretastatin and the hCE1-sensitive motif (Scheme 1). For the synthesis of colchicine C_{10} derivatives, we chose the synthetic approaches provided in Scheme 2, using colchicine as starting material. Modifications included substitution of the methoxy group with amino functionalities (ammonia or amino acid derivatives) at position 10. The formed 10-aminocolchicine or its derivatives were subjected to further transformations via coupling reactions with the hCE1-sensitive motif to obtain the final compounds (Scheme 2). The spacers connecting the 10-aminocolchicine molecule to the hCE1-sensitive motif were chosen to convey higher hydrophobicity to the esters and thereby facilitate its penetration through the cellular membrane and interaction with the hydrophobic pocket of the colchicine-binding site.

Cytotoxicity assay

Cytotoxicity of the studied compounds was evaluated by Cell Titer Blue assay in HeLa and Huh7 cell lines over periods of 24

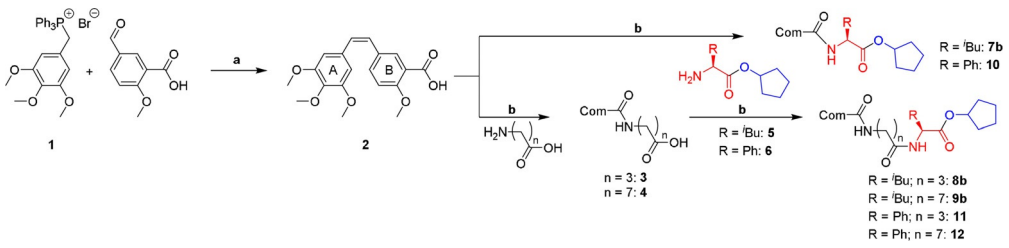

Scheme 1. Synthesis of B-3-combretastatin derivatives: Combretastatin carboxylic acid (**2**) was formed in a Wittig reaction between the phosphonium salt **1** and the aromatic aldehyde. The coupling of the amino acid cyclopentyl ester and—if applicable—the alkyl spacer was performed in solution with the coupling reagent 1-[bis(dimethylamino)methylene]-1*H*-1,2,3-triazolo-[4,5-*b*]pyridinium-3-oxide hexafluorophosphate. Reagents and conditions: a) BuLi, THF, 0 °C→RT, 12 h; b) HATU, DMF, 0 °C→RT, 24 h. The structural element of the amino acid (phenylglycine or leucine) is marked in red, cyclopentanol in blue.

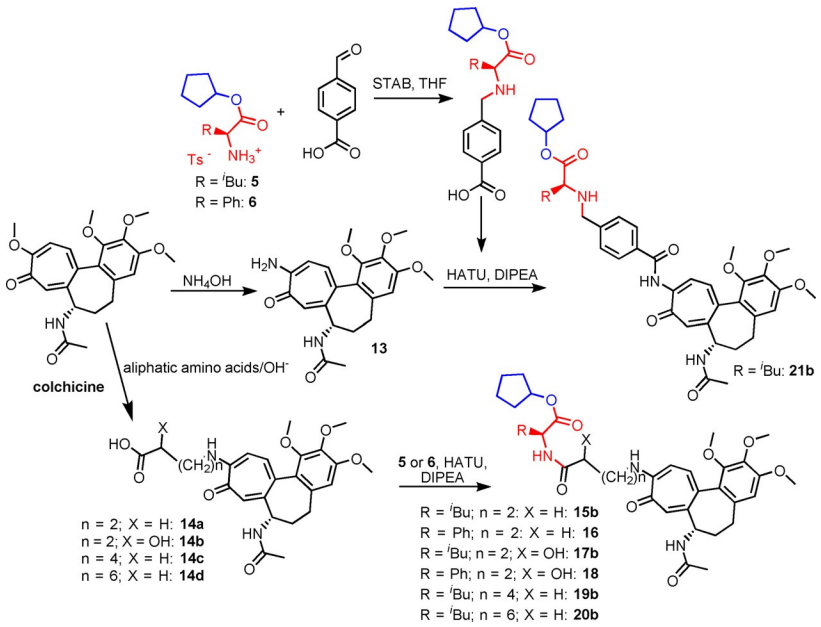

Scheme 2. Synthesis of C_{10}-colchicine derivatives.

and 72 h. Attempts to measure the cytotoxicity in a 24 h assay did not show the full cytotoxic effect of combretastatin, colchicine and its derivatives.

The main objective in creating prodrugs was to decrease the cytotoxicity of combretastatin and its derivatives. Indeed, all obtained derivatives show a cytotoxicity of at least three orders of magnitude lower than combretastatin A-4. The prodrug with a leucine cyclopentanol ester linked to combretastatin (**7b**) already shows a large decrease in toxicity with a CC_{50} at about 30 μM. If there is a spacer with a length of four carbon atoms (4-aminobutyric acid) inserted between combretastatin and the hCE1-sensitive motif (**8b**), the compounds become slightly more toxic, perhaps due to higher permeability or stability. However, the analogue with a C_8 spacer (**9b**) shows reduced toxicity. We observed the same characteristics with the phenylglycine cyclopentanol esters **10**, **11** and **12**.

Analysis of the data of colchicine derivatives obtained in 72 h treatment period shows that all 10-aminocolchicine derivatives appear at least 100-fold less toxic than the initial 10-aminocolchicine and colchicine. These data correlate very well with the results obtained by other researchers that demonstrated lower toxicity of the 10-alkylaminocolchicine derivatives as compared to 10-aminocolchicine and colchicine.[38,39] In conclusion, the aim of reduced toxicity was achieved by creation of prodrugs for colchicine and combretastatin.

Tubulin polymerization inhibition by combretastatin and colchicine derivatives and its correlation with antiviral activity

The antiviral activity against DENV was measured after a 24 h incubation period with compound concentrations that allowed cell viabilities greater than 80%. However, after 72 h incubation, cytotoxicity was observed in the nanomolar concentration range for the initial compounds (colchicine, combretastatin) and in the micromolar range for the derivatives. Along with the cytotoxicity, the ability of these compounds to inhibit the polymerization of tubulin drops with increasing length of the spacer. At a concentration of 10 μM, prodrug **7b** leads to a tubulin polymerization grade of 88% compared with the DMSO control (Table 1). Prodrug **8b** with the 4-aminobutyric acid spacer showed almost no inhibition (95% polymerization grade), while the most bulky prodrug **9b** seems to promote tubulin polymerization. Although this compound might act as microtubule stabilizer like paclitaxel, it is more likely that it either leads to precipitation of tubulin or precipitates itself and thereby generated a false-positive signal in the tubulin polymerization assay.

The same correlation between the length of the spacer and the potency to inhibit tubulin polymerization is observed with the phenylglycine cyclopentanol esters **10**, **11** and **12**. Yet, these compounds show overall higher polymerization inhibition, with **11** being the most active one, reducing the rate of tubulin polymerization to 60%. After hydrolysis, the toxicity of the hydrolyzed peers **7a**, **8a** and **9a** is lower than in their precursors, perhaps because of pharmacokinetic effects, such as lower permeability of the carboxylate.

The hydrolyzed prodrugs show similar effects on tubulin polymerization as their precursors. For the pair **8a/b**, a moderate increase in activity could be found after hydrolysis. Nevertheless, the concept of intracellular prodrug cleavage by ester hydrolysis does not require an increase of activity, because the hydrolyzed carboxylate drug can be anticipated to have low passive membrane permeability and thereby accumulate in the target cell.

The hydrolyzed analogues of the colchicine prodrugs with shorter spacers like γ-amino-β-hydroxybutyric and γ-aminobutyric acid are less active in the tubulin polymerization assay

Table 1. Combretastatin and colchicine derivatives: effect on tubulin polymerization, cytotoxicity, and susceptibility to hCE1-catalyzed hydrolysis.

Compound	Structure[a]	Polymerization [%][b]	CC_{50} [μM] (72 h) HeLa	CC_{50} [μM] (72 h) Huh7	Cleavage [%][c]
DMSO		100	–	–	–
combretastatin A-4	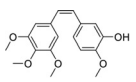	40 ± 4	0.003 ± 0.001	0.009 ± 0.002	n.a.
2	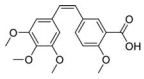	91 ± 2	> 50	> 50	n.a.
7a	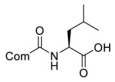	88 ± 2	63.99 ± 1.68	> 50	n.a.
7b	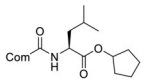	88 ± 5	39.67 ± 1.45	26.05 ± 2.45	63.32 ± 2.11
8a	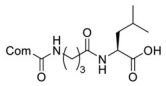	84 ± 8	> 50	> 50	n.a.
8b	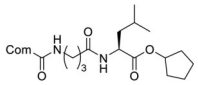	95 ± 2	0.92 ± 0.63	14.99 ± 1.73	68.16 ± 3.24
9a	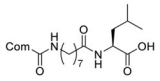	112 ± 5	26.65 ± 2.59 μM	> 50	n.a.
9b	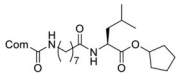	142 ± 22	5.07 ± 4.16	22.04 ± 1.55	38.11 ± 4.64
10	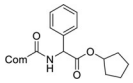	79.4 ± 1.0	6.83 ± 2.23	8.52 ± 1.54	0
11	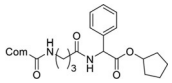	60 ± 2	0.95 ± 0.72	4.60 ± 1.26	0
12	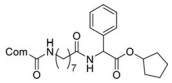	93 ± 6	> 50	11.39 ± 1.66	0
colchicine	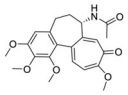	22 ± 8	0.058 ± 0.004	0.003 ± 0.002	n.a.
13	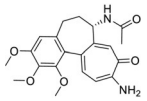	33 ± 2	0.007 ± 0.005	0.008 ± 0.004	n.a.
15a	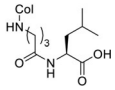	106 ± 4	> 50	> 50	n.a.
15b	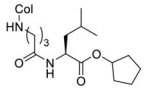	86 ± 6	1.19 ± 0.89	2.79 ± 1.25	17.99 ± 1.46
16	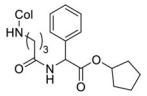	71 ± 11	1.24 ± 0.86	5.40 ± 1.51	0
17a	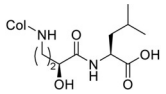	120 ± 9	0.96 ± 0.72	3.27 ± 1.47	n.a.
17b	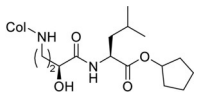	95 ± 5	0.23 ± 0.16	0.68 ± 0.42	13.33 ± 0.34
18	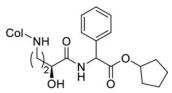	110 ± 6	0.22 ± 0.15	0.62 ± 0.39	0

Table 1. (Continued)

Compound	Structure[a]	Polymerization [%][b]	CC_{50} [μM] (72 h) HeLa	Huh7	Cleavage [%][c]
19a	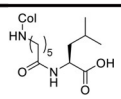	88 ± 5	1.07 ± 0.85	1.19 ± 0.81	n.a.
19b	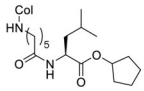	97 ± 1	4.62 ± 1.71	6.08 ± 1.66	35.70 ± 3.25
20a	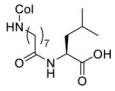	103 ± 3	> 50	> 50	n.a.
20b	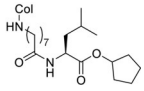	100 ± 1	4.93 ± 1.85	4.48 ± 1.74	76.24 ± 11.56
21a	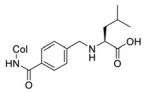	92 ± 4	0.73 ± 0.50	1.17 ± 0.78	n.a.
21b	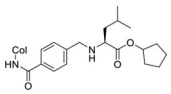	118 ± 17	1.48 ± 1.06	4.95 ± 0.28	32.64 ± 5.37

[a] Com: combretastatin residue, Col: colchicine residue. [b] Conditions for tubulin polymerization assays: 4 mg mL^{-1} tubulin, 1 mM GTP, 10 μM test compound, 80 mM PIPES, pH 6.9, 0.5 mM EGTA, 2 mM $MgCl_2$, 1 h, 37 °C; values represent the degree of polymerization relative to DMSO blank (100%: no inhibition). All experiments were performed in triplicate. [c] Hydrolysis assay: [hCE1] = 100 nM, [test compound] = 10 μM in phosphate buffer, pH 7.4, incubated for 2 h at 37 °C (if no cleavage was observed under these conditions, then the incubation was repeated for 24 h). All experiments were performed in triplicate; n.a.: not applicable (i.e., molecule has no cleavage site).

than the respective prodrugs, possibly because of higher polarity of the residue at position 10 relative to other colchicine derivatives. This property is probably not compatible with binding to hydrophobic regions in the colchicine-binding site. The only colchicine derivative for which its hydrolyzed peer has shown higher inhibitory activity on tubulin polymerization than the initial prodrug was compound **21b**. In this case the polarity of the carboxylic group in the motif is counterbalanced by the nonpolar aromatic ring.

The fact that toxicity and activity of the microtubule disrupting agents have been assayed in tumor cell lines might bring one artefact interaction that would be avoided in healthy cells. Thus, the possible interaction of the obtained compounds with the membrane-bound P-glycoprotein (P-gp, ABCB1, MDR1), which is overexpressed in several different tumor types and is associated with poor response to chemotherapy (various microtubule disrupting compounds are substrates for P-gp, and colchicine is one of them), might be one of the effects that could influence the cell viability and antiviral response. However, it has been detected before[52] that minimal size of the colchicine derivative molecule is important for the interaction with P-gp, which means that derivatization with larger substituents can affect it. According to Tang-Wai et al.[52] the presence of rings B and C is also crucial, which means that colchicine's biphenyl analogues, like combretastatin, lack this interaction.

Combretastatin, colchicine and some of the colchicine derivatives were tested on their antiviral activity against dengue and Zika virus (Table 2). The activity (EC_{50}) of combretastatin and colchicine against dengue replication was 870 nM, and 150 nM, respectively. The colchicine prodrug **21b** showed considerable antiviral activity despite its marginal effect on tubulin polymerization, possibly due to an effect on microtubule dynamics or due to interactions with other host cellular or viral mechanisms.

Hydrolysis of combretastatin and colchicine derivatives by hCE1

The active site cavity of hCE1 is very large (≈1300 Å^3 in volume), mostly flexible and is lined mainly by hydrophobic residues, with the exception of the catalytic triad. The enzyme is therefore considered to be relatively promiscuous and capable of interacting with a variety of diverse ligands[53] preferring those with small alcoholic group and a bulky acyl group, such as oseltamivir, clopidogrel[54] and enalapril.[55]

Nevertheless, a clear structure-cleavability-relationship for hCE1 substrates is observed in the present study. All combretastatin prodrugs that contain the leucine cyclopentyl moiety were hydrolyzed by the carboxyl esterase (Table 1). High-resolution ESI mass spectrometry detected the resulting carboxylic acids and the ratio of hydrolyzed prodrug was quantified by HPLC-UV. The conversion was less effective for derivatives containing a long alkyl spacer. The 8-aminooctanoic acid analogue (**9b**) had the lowest ratio of cleavage. This might be due to steric hindrance by the C_8 chain. The prodrugs with a 4-aminobutyric acid based spacer and with no spacer at all were

Table 2. Antiviral activity in Huh7 cells against DENV or ZIKV.

Compound	Structure[a]	CC_{50} [μM] (24 h)	Virus titer reduction[b]
combretastatin A-4	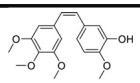	38.30	DENV: EC_{50} = 870 nM ZIKV: 70% at 5 μM
colchicine	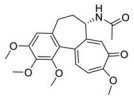	29.91	DENV: EC_{50} = 150 nM ZIKV: 89.67% at 5 μM
13	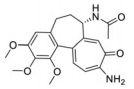	16.84	DENV: 37.04% at 0.78 μM
17b	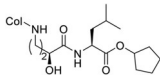	32.54	ZIKV: EC_{50} = 878 nM
19b	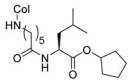	16.25	DENV: 20.00% at 3.125 μM
20b	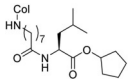	8.95	DENV: 40.00% at 3.125 μM
21b	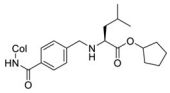	10.98	DENV: 52.94% at 0.78 μM ZIKV: EC_{50} = 1.851 μM

[a] Com: combretastatin residue, Col: colchicine residue. [b] Given is either the percent virus titer reduction at a certain concentration, or the concentration at which virus titer was reduced by 50% (EC_{50}), determined after an exposure time of 24 h; for the sake of comparison, the CC_{50} values in Huh7 cells at 24 h are provided.

cleaved more effectively. Conversion rates after 1 h of incubation were between 60–70%.

On the other hand, all phenylglycine cyclopentyl ester combretastatins were inert against hydrolysis by hCE1. This contradicts the results by Needham et al.[21] who presented the phenylglycine cyclopentyl moiety as an hCE1 sensitive motif. After incubation, no cleavage products could be detected by HPLC-UV or ESI-MS.

Out of all colchicine derivatives with esterase-sensitive motifs tested for cleavability, only those containing leucine cyclopentyl ester were hydrolyzed by hCE1. In the row of derivatives with spacers ranging from γ-aminobutyric acid to ε-aminocaproic acid and 8-aminooctanoic acid the average conversion rate increased from 17.99 ± 1.46% to 35.70 ± 3.25% and 76.24 ± 11.56%, respectively. Hydrolysis could not be observed for the phenylglycine cyclopentyl esters moieties. As for the combretastatin analogues, the lack of hydrolysis of the phenylglycine cyclopentyl ester by hCE1 is in conflict with the data presented by Needham et al.[21]

Considering this conflicting evidence, we studied whether compounds with the Phg-Cyp motif inhibit the hydrolytic activity of hCE1. Compounds **10**, **11**, **12** and **18** were therefore assayed for inhibition of hCE1 activity. However, these compounds did not reduce the hydrolysis of the substrate *p*-nitrophenyl acetate by hCE1.

Another possible reason for the lack of the derivatives' hydrolysis was the inability of their ester moieties to enter the hydrolytic site of the enzyme, which could have been caused by racemization of the Phg that has been previously detected in similar conditions of solid-phase peptide synthesis[56] or steric hindrance as it could be in the case of *tert*-butyl derivatives.[20] However, one of the stereoisomers should still fit the enzyme hydrolytic pocket and, at least, partial hydrolysis should take place. Only 4-formylbenzoic acid based spacer in colchicine derivatives gave the prodrugs that are inactive before cleavage and get activated after cleavage. Introduction of alkyl spacers resulted in compounds with good inhibition of tubulin polymerization in uncleaved form lower inhibition in cleaved form. Remaining uncleaved and active these compounds cannot be classified as prodrugs but only as active compounds.

Molecular modelling studies

To rationalize the binding mode of the compounds, docking of some of them was performed in the colchicine-binding site of tubulin. Initially, the parent compounds combretastatin (Com) and colchicine (Col) were docked into the colchicine-binding site of tubulin to validate the docking procedure.

The protonated ligand structures were optimized within the binding site in the crystal structure of tubulin (PDB ID: 4O2B for the Col derivatives,[57] and PDB ID: 5LYJ for the Com derivatives[24]). In the process of docking, the active site around the bound inhibitor in the molecular structure of tubulin was determined with the radius of 8 Å. Values of free energies of binding between the protein and the ligand were calculated taking into account the contributions of hydrogen bonds, as well as ionic, hydrophobic and van der Waals interactions.

The predicted energies of binding between the protein and Col or Com were 16.84 kcal mol^{-1} and 15.12 kcal mol^{-1}, respec-

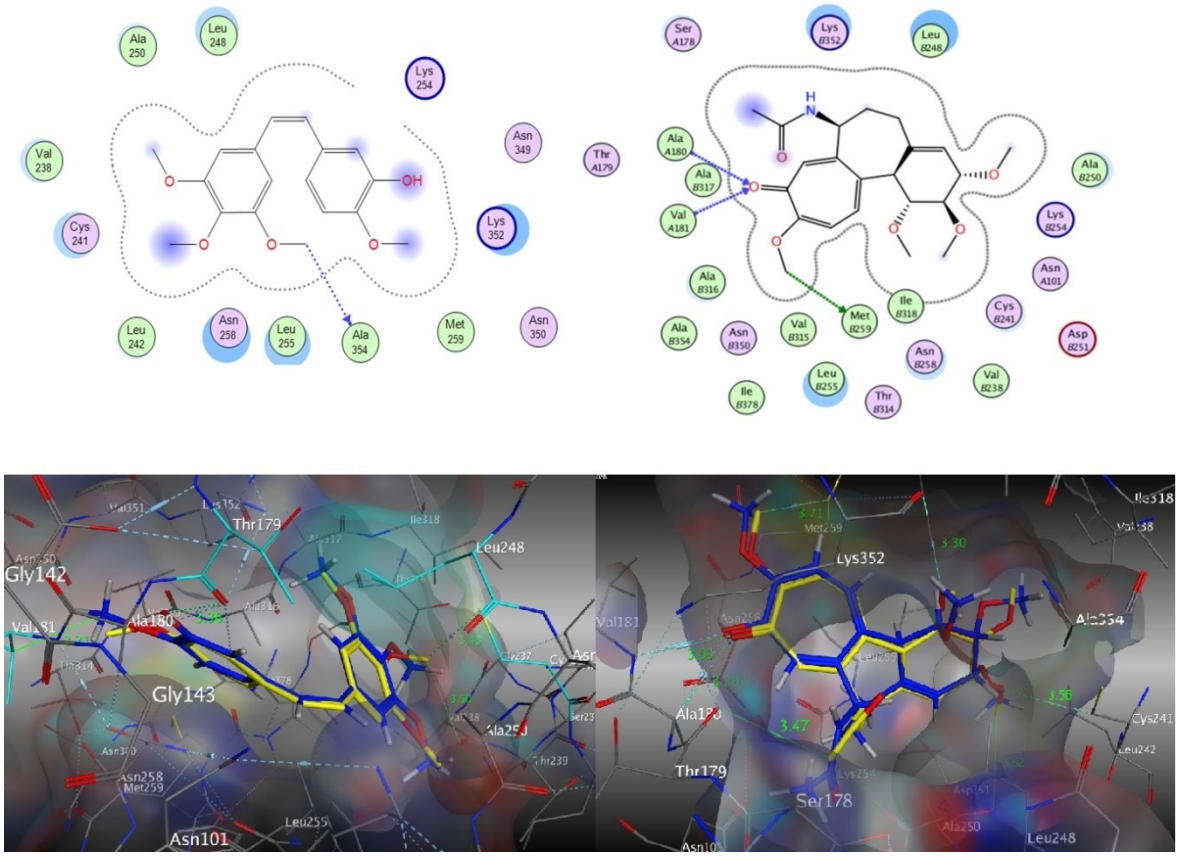

Figure 4. 2D diagram (ligand interactions) and 3D interactions with the tubulin binding site for Col (right) and Com (left). Blue shows the position of ligands taken from crystal structures PDB ID: 4O2B and PDB ID: 5LYJ.

tively, which is in accordance with their inhibiting effect on the polymerization of tubulin. The best docking positions for Col (right) and Com (left) with amino acid residues of the active site are shown in Figure 4.

The performed docking calculations are in agreement with the experimental X-ray structures. This indicates a correct choice of parameters for docking and the force field calculations. Let us briefly consider some features of the interaction of the base molecules Com and Col that is important for further analysis of the results of docking in regard of their derivatives. As can be seen from the results of docking, both molecules bind to the colchicine-binding site via hydrogen bonds and hydrophobic interactions. The molecule Col is orientationally fixed in a hydrophobic pocket consisting of Val181α (3.05 Å) and Ala180α (3.26 Å). The stabilization of the Col molecule is due to the H-bond acceptor interaction with the carbonyl group of the seven-membered ring of colchicine. The H-bond donor interaction is observed between the amino acid residues Met259β (3.71 Å), Thr179α (3.47 Å) and the methoxytropone ring. The 3- and 4-methoxyphenyl groups can form hydrogen bonds with Cys241β (3.56 and 4.68 Å).

Com binding also occurs in the colchicine-binding site of tubulin, with the only difference that amino acid residues taking part in the formation of the ligand–protein complex are a bit different (Figure 4, bottom). The molecule Com is loosely located in the pocket of tubulin and forms strong hydrophobic interactions with residues Leu248β, Ala354β and Val181α of the active center of the protein. As seen from Figure 4, the strong binding of compounds to the protein determines their inhibiting activity as to the polymerization of tubulin that corresponds to the experimental results of the studies on the inhibition of tubulin polymerization.

The next step in molecular modelling was to study the binding mode of the Com and Col derivatives to tubulin. To this end, we examined the docking of the molecules **8a**, **17a** and **21a** which are representatives of the synthesized series of the Com and Col basic structures, to the colchicine-binding site of tubulin.

The increase in size and volume of the molecule directly affects the character of binding to the receptor. Figure 5 presents a 2D diagram and the 3D arrangement of molecules bound to the colchicine-binding site of tubulin. As can be seen from Figure 5, several binding interactions different from Com appear between the Com derivative **8a** and the amino acid residues of the active site. For example, the formation of a strong hydrogen bond between Asn349β (2.27 Å) and the hydroxy group is observed in the 4-aminobutyric acid fragment.

At the opposite end of the molecule, a new close contact appears between the 3-methoxy group of **8a** and the carbonyl group of Cys241β (2.75 Å) and Val238β (3.03 Å). It should be noted that the interaction with the receptor occurs predominantly through the β-subunit of the protein. Hydrophobic in-

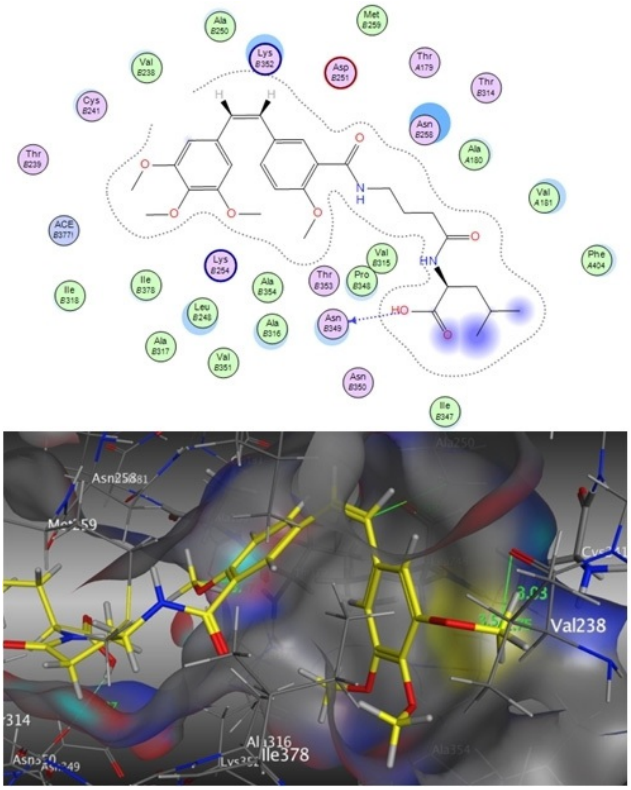

Figure 5. 2D diagram and 3D interactions with the tubulin binding site for **8a**.

teractions of the molecule at distances from 3.47 to 3.95 Å arise with Lys352β, Ala354β, Thr179α, and Val181α. The predicted binding energy of **8a** with the target is 10.37 kcal mol^{-1}, considerably lower than for Com. This suggests a weaker interaction of **8a** with the target.

The results of docking of the Col derivative **17a** compound are shown in Figure 6. As seen from the 2D diagram, the molecule forms several hydrogen bonds with the target. The strongest interaction is observed for Glu183α (2.41 Å) and Pro173α (1.79 Å). Similar to **8a**, the main contributions to the binding arise from the terminal parts of the molecule (4-aminobutyric acid and 3,4,5-trimethoxyphenyl-methoxytropone ring). Formation of the hydrogen bond Pro173α with the acetamide group of the seven-membered ring is characteristic for **17a**.

The linker (-CH_2-)$_n$ attached to the acetamide group does not radically affect the character of binding of the root (head) part of the molecule (Col and Com) to the active site of the protein. Differences are observed in the spatial arrangement of these molecules in the receptor pocket and in their specific binding to the amino acids of the protein. All this leads to a decrease in predicted energy of binding to the target for **17a** (11.27 kcal mol^{-1}), compared to the unsubstituted molecule (Col −16.84 kcal mol^{-1}).

The exit of a bulk molecule from the colchicine-binding site can be one of the factors reducing the inhibitory activity of the molecule as to the tubulin polymerization, and in some cases (see **9a** and **17a**) it can even accelerate its polymerization. The introduction of the phenyl group into the base

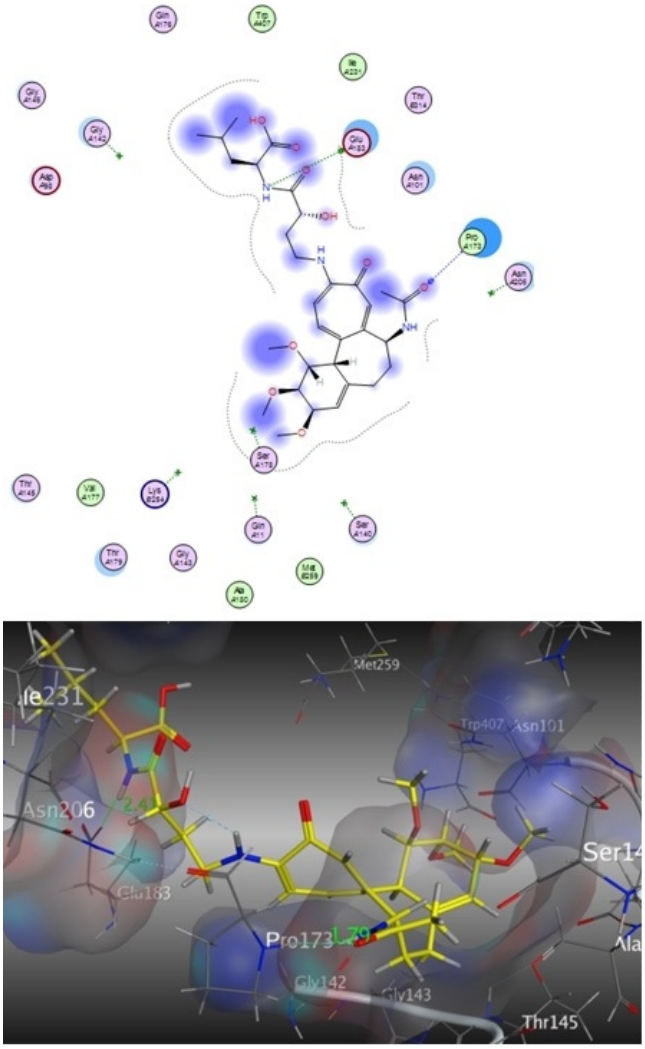

Figure 6. 2D diagram and 3D interactions with the tubulin binding site for **17a**.

molecule as a linker is illustrated by the example of the Col derivative **21a**. The docking pose of **21a** in the binding site of tubulin is shown in Figure 7.

As in the case of **17a**, the H-bond acceptor interactions of the amide group (-NH-) with Glu183α (2.45 Å) and of the 4-methoxy groups with Tyr224α (2.62 Å) are observed for **21a**. The hydrogen bond formation with participation of the amide fragment is characteristic for most compounds exhibiting biological activity. The aromatic ring does not participate in direct binding to the receptor.

On the other hand, as noted above, the linker can significantly affect the spatial orientation of a ligand. Due to the presence of the conformationally flexible alkyl linkers (-CH_2-)$_n$, the possibility of changing the spatial orientation of the head (Col and Com) and tail (4-aminobutyric acid) of the molecule increases significantly (see **8a**, **9a**, and **17a**). The addition of the "hard" phenyl ring to the Col molecule makes the **21a** compound more flat and stiff, due to the presence of the stabilizing π-bonds in the Col-NH-CO-Ph fragment. The predicted

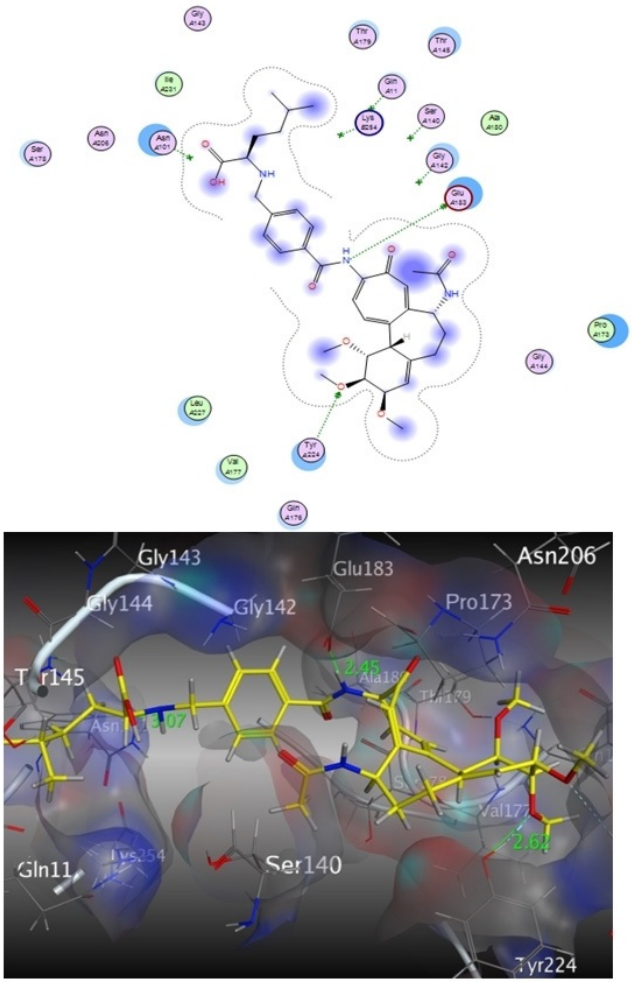

Figure 7. 2D diagram and 3D interactions with the tubulin binding site for **21 a**.

energy of binding with the target for both **21 a** and **17 a** amounts to 11.25 kcal mol^{-1}, and is significantly lower than for Col.

In conclusion, it should be noted that the Col and Com derivatives obtained in this work form less interactions with the colchicine-binding site of tubulin and inhibit the polymerization of the protein to a lesser extent. At the same time, they are less toxic than non-substituted Col and Com.

Conclusions

The main pharmacological property and disadvantage of the TPIs regarding their use for antiviral therapy is their high cytotoxicity. As a result of the designed modifications in the structure of two TPIs, colchicine and combretastatin, a group of less toxic derivatives with an hCE1-sensitive motif in their structure was obtained. It could be demonstrated that only Leu-based derivatives were subjected to hydrolysis by hCE1 whereas the Phg-containing analogues remained uncleaved, in contrast to the findings of Needham et al.[21] The Leu- and Phg-based derivatives were less cytotoxic than their parent compounds colchicine and combretastatin. Docking studies of the compounds within the colchicine-binding site of tubulin indicated several reasons for the lower affinity toward tubulin. The most active compounds in viral replication assays were the parent compounds colchicine and combretastatin, but some derivatives like **21 b** and **17 b** also showed good activity while being much less toxic. The lack of correlation between tubulin binding, cytotoxicity and the antiviral activity of the initial compounds and their derivatives indicates that tubulin binding is not the only mechanism of antiviral activity of the latter. Moreover, the lack of significant difference between the cytotoxicity of cleavable and non-cleavable compounds indicates that the hCE1 selective motif does not influence the toxicity. Further exploration of this topic could elucidate alternative mechanisms of antiviral activity of the obtained derivatives besides tubulin binding.

Experimental Section

Chemistry: All chemicals for the synthesis were of analytical grade and purchased from Sigma–Aldrich (Germany), Carbolution (Germany), TCI (Belgium), Carl Roth GmbH (Germany), and Acros Organics (Belgium). Chemicals were used without further purification unless otherwise stated. All solvents were purchased from commercial sources. Dry solvents were stored over molecular sieves. NMR spectra were recorded on a Varian NMR instrument at 300 MHz, 298 K in $CDCl_3$, CD_3OD or [D_6]DMSO. Chemical shifts (δ) are given in parts per million (ppm). Proton peaks of residual non-deuterated solvents were used for calibration. Coupling constants (J) are given in Hertz (Hz). Multiplicity is given as s (singlet), d (doublet), t (triplet), q (quartet) or m (multiplet). Mass spectra were measured on a Bruker micrOTOF-Q II (HR-ESI) instrument. Flash chromatography was performed on a Biotage Isolera One purification system using silica gel (0.060–0.200 mm) cartridges (KP-Sil) and UV monitoring at 254 nm and 280 nm. Preparative HPLC was performed on an ÄKTA Purifier, GE Healthcare (Germany), with an RP-18 pre and main column (Reprospher, Dr. Maisch GmbH, Germany, C18-DE, 5 μm, 30 mm × 16 mm and 120 mm × 16 mm). Analytical HPLC was performed on an Agilent 1200 HPLC system with a UV detector on an RP-18 column (ReproSil-Pur-ODS-3, Dr. Maisch GmbH, Germany, 3 μm, 50 mm × 2 mm).

Synthesis of 1: 3,4,5-Trimethoxybenzaldehyde (3 g, 15.3 mmol, 1 equiv) was dissolved in 50 mL MeOH. $NaBH_4$ (1.17 g, 30.6 mmol, 2 equiv) was added in portions. The solution was stirred for 30 min at room temperature. Upon completion, the solvent was removed under reduced pressure and the residue was dissolved in dichloromethane, washed with H_2O, dried over $MgSO_4$ and concentrated in vacuo. Yield 2.44 g (12.32 mmol, 81 %). ^{1}H NMR ($CDCl_3$): δ = 6.61 (s, 2 H), 4.64 (d, J = 4.4 Hz, 2 H), 3.87 (s, 6 H), 3.84 (s, 3 H), 1.64 (t, J = 4.4 Hz, 1 H).

(3,4,5-Trimethoxyphenyl)methanol (2.4 g) was dissolved in 100 mL dichloromethane and cooled to 0 °C. PBr_3 (1.25 mL, 13.3 mmol, 1.1 equiv) was added dropwise. The solution was stirred for 30 min. Upon completion, the reaction was quenched with ice-cold H_2O and the product was extracted with dichloromethane. The combined organic extracts were dried over $MgSO_4$ and concentrated in vacuo. Yield 2.7 g (10.4 mmol, 86 %). ^{1}H NMR ($CDCl_3$): δ = 6.62 (s, 2 H), 4.46 (s, 2 H), 3.87 (s, 6 H), 3.84 (s, 3 H).

In a round-bottom flask, 2.7 g (10.4 mmol, 1 equiv) 3,4,5-trimethoxybenzylbromide and 2.7 g (10.4 mmol, 1 equiv) PPh_3 were dissolved in chloroform. The solution was held at reflux at 65 °C for

24 h. The solvent was removed under reduced pressure. The oily residue was collected in cyclohexane and evaporated again, yielding a white solid. The crude product was purified by recrystallization in EtOH. Yield 5.4 g (10.4 mmol, 100%). ^{1}H NMR ($CDCl_3$): δ = 7.80–7.73 (m, 9H), 7.66–7.62 (m, 6H), 6.46 (d, J = 2.7 Hz, 2H), 5.40 (d, J = 13.9 Hz, 2H), 3.76 (s, 3H), 3.51 (s, 6H).

General procedure for Wittig reaction of combretastatin A-4 and 2: In a dry and nitrogen-purged round-bottom flask, 500 mg (0.955 mmol, 2 equiv) **1** were suspended in 10 mL dry THF and cooled to 0 °C. 955 μL (2.38 mmol, 5 equiv) of a 2.5 M *n*-butyllithium solution in hexane were added dropwise. The suspension should maintain an orange color for at least 30 min. Then, the corresponding benzaldehyde (0.477 mmol, 1 equiv) was added in one portion. The reaction mixture was allowed to warm to room temperature and stirred overnight. Upon completion, the reaction was quenched with ice-cold H_2O. The aqueous phase was neutralized with 1 M HCl and the product was extracted three times with EtOAc. The combined organic extracts were dried over $MgSO_4$ and evaporated to give the crude product that contained the *cis* and *trans* isomers. The desired *cis* product (combretastatin A-4) or a mixture of *cis* and *trans* product, respectively (**2**) was isolated by flash chromatography (10–60% EtOAc in cyclohexane for combretastatin A-4 and 10% MeOH in EtOAc for **2**).

Combretastatin A-4: Yield 56 mg (0.177 mmol, 37%). ^{1}H NMR ($CDCl_3$): δ = 6.92 (d, J = 1.8 Hz, 1H), 6.79 (dd, J = 8.3 Hz, J = 1.8 Hz, 1H), 6.73 (d, J = 8.3 Hz, 1H), 6.52 (s, 2H), 6.47 (d, J = 12.1 Hz, 1H), 6.41 (d, J = 12.1 Hz, 1H), 5.52 (br s, 1H), 3.86 (s, 3H), 3.84 (s, 3H), 3.70 (s, 6H); HRMS-ESI (*m/z*): $[M+Na]^+$ calcd for $C_{18}H_{20}O_5Na$: 339.1203, found: 339.1210.

2: Combined yield 96.6 mg (0.281 mmol, 59%). ^{1}H NMR ($CDCl_3$): *cis* isomer: δ = 8.15 (d, 2.0 Hz, 1H), 7.45 (dd, J = 8.8 Hz, J = 2.0 Hz, 1H), 6.89 (d, J = 8.8 Hz, 1H), 6.57 (d, J = 12.1 Hz, 1H), 6.50 (d, J = 12.1 Hz, 1H), 6.45 (s, 2H), 4.05 (s, 3H), 3.85 (s, 3H), 3.69 (s, 6H). *trans* isomer: δ = 8.37 (d, J = 2.0 Hz, 1H), 7.68 (dd, J = 8.6 Hz, J = 2.0 Hz, 1H), 7.07 (m, 1H), 7.06 (d, J = 16.6 Hz, 1H), 6.97 (d, J = 16.6 Hz, 1H), 6.74 (s, 2H), 4.11 (s, 3H), 3.92 (s, 6H), 3.87 (s, 3H); HRMS-ESI (*m/z*): $[M+Na]^+$ calcd for $C_{19}H_{20}O_6Na$: 367.1158, found: 367.1186.

General procedure for amide coupling of compounds (3, 4, 7b, 8b, 9b, 10, 11, 12): In a dry round-bottom flask, 1 equiv carboxylic acid, 1.05 equiv 1-[bis(dimethylamino)methylene]-1*H*-1,2,3-triazolo-[4,5-*b*]pyridinium-3-oxide hexafluorophosphate (HATU) and 1.1 equiv 1-hydroxy-7-azabenzotriazole (HOAt) were dissolved in 3 mL dry DMF. The solution was cooled to 0 °C and 1.3 equiv diisopropylethylamine (DIPEA) were added. The resulting yellow solution was stirred for 3 min, then 1 equiv amine was added and the reaction was stirred overnight at room temperature. After completion, the reaction was quenched with ice and the solvent was evaporated in vacuo. The residue was purified by preparative HPLC (10–80% MeOH in H_2O).

3 HRMS-ESI (*m/z*): $[M+Na]^+$ calcd for $C_{23}H_{27}NO_7Na$: 452.1680, found: 452.1680. **4** HRMS-ESI (*m/z*): $[M+Na]^+$ calcd for $C_{27}H_{35}NO_7Na$: 508.2311, found: 508.2497. **7b** HRMS-ESI (*m/z*): $[M+Na]^+$ calcd for $C_{30}H_{39}NO_7Na$: 548.2619, found: 548.2602. **8b** HRMS-ESI (*m/z*): $[M+Na]^+$ calcd for $C_{34}H_{46}N_2O_6Na$: 633.3146, found: 633.3171. **9b** HRMS-ESI (*m/z*): $[M+Na]^+$ calcd for $C_{38}H_{54}N_2O_8Na$: 689.3772, found: 689.3775. **10** HRMS-ESI (*m/z*): $[M+Na]^+$ calcd for $C_{32}H_{35}NO_7Na$: 568.2306, found: 568.2285. **11** HRMS-ESI (*m/z*): $[M+Na]^+$ calcd for $C_{36}H_{42}N_2O_8Na$: 653.2833, found: 653.2863. **12** HRMS-ESI (*m/z*): $[M+Na]^+$ calcd for $C_{40}H_{50}N_2O_8Na$: 709.3459, found: 709.3457.

Synthesis of the hCE1-sensitive motif tosylate salt of cyclopentyl L-leucinate (5): Cyclopentanol (28.00 mL, 305 mmol) and *p*-toluenesulfonic acid (6.43 g, 33.3 mmol) were added to a suspension of L-leucine (4.062 g, 30.5 mmol) in cyclohexane (150 mL). The vessel was fitted with a Dean–Stark receiver and slowly heated to 120 °C for complete dissolution of the reactants. Temperature was maintained at 120 °C for a period of 12 h. The reaction was then cooled to room temperature, which lead to precipitation of a white solid. The solid was filtered and washed with EtOAc before drying in vacuo using a desiccator. Yield 9.630 g (85%); ^{1}H NMR (300 MHz, [D_6]DMSO, δ/ppm, *J*/Hz): 7.63–7.77 (m, 2H, tosyl protons), 7.23 (dd, J = 8.7, 0.7, 2H, tosyl protons), 5.26–5.32 (m, 1H), 3.95 (t, J = 6.9, 1H), 2.37 (s, 3H), 1.85–2.00 (m, 2H), 1.60–1.83 (m, 8H, cyclopentyl protons), 0.99 (dd, J = 5.8, 6H, leucine); HRMS-ESI (*m/z*): $[M+H]^+$ calcd for $C_{11}H_{21}NO_2$: 200.1645, found: 200.1700.

Synthesis of the hCE1-sensitive motif chloride salt of cyclopentyl L-phenylglycinate (6): To a slurry of L-phenylglycine (3.054 g, 20 mmol) in cyclopentanol (20 mL) in an ice bath, thionyl chloride (5.19 mL, 70 mmol) was added dropwise over a period of 5 min from an automatic pipette with a polyethylene tip. The resulting mixture was kept at 0 °C for approximately 15 min before it was gently heated to 120 °C (using an oil bath) for 12 h. Then it was left overnight at RT for crystallization. The solid was filtered and washed with EtOAc before drying in vacuo in a desiccator. Yield 1.910 g (37%); ^{1}H NMR (300 MHz, [D_6]DMSO, δ/ppm, *J*/Hz): 8.99 (br s, 3H, NH_3^+), 7.37–7.53 (m, 5H, phenyl), 5.13–5.20 (m, 2H), 1.31–1.94 (m, 8H, cyclopentyl protons); HRMS-ESI (*m/z*): $[M+H]^+$ calcd for $C_{13}H_{18}NO_2$: 220.1332, found: 220.1378.

General procedure for synthesis of metabolites (7a, 8a, 9a). In a round-bottom flask, 1 equiv free carboxylic acid, 1.05 equiv HATU and 1.1 equiv HOAt were dissolved in 3 mL dry DMF. The solution was cooled to 0 °C and 2.3 equiv diisopropylethylamine (DIPEA) were added. The resulting yellow solution was stirred for 3 min, then 1 equiv L-leucine *tert*-butyl ester hydrochloride was added and the reaction was stirred overnight at room temperature. After completion, the reaction was quenched with ice. The resulting precipitate was filtered and dissolved in a 1:1 mixture of CH_2Cl_2 and TFA. This solution was stirred for 15 min at room temperature, and then the solvents were removed in vacuo. The residue was purified by preparative HPLC (10–80% MeOH in H_2O).

7a HRMS-ESI (*m/z*): $[M+Na]^+$ calcd for $C_{25}H_{31}NO_7Na$: 480.1993, found: 480.1989. **8a** HRMS-ESI (*m/z*): $[M-H]^-$ calcd for $C_{29}H_{37}N_2O_8$: 541.2555, found: 541.2557. **9a** HRMS-ESI (*m/z*): $[M-H]^-$ calcd for $C_{33}H_{45}N_2O_8$: 597.3170, found: 597.3173.

Synthesis of 10-demethoxy-10-aminocolchicine (13). 0.399 g (1 mmol) of colchicine were mixed with 2 mL of NH_4OH 25% and 0.5 mL of 96% EtOH. The mixture was placed in a 10 mL microwave reaction tube and placed for 15 min, at 110 °C and 1200 rpm in a microwave reactor. After that it was checked by TLC, diluted with H_2O and extracted with EtOAc. The extract was dried over $MgSO_4$, filtered and resulting solution checked by TLC again. Afterward, the compound was purified by flash column chromatography with evaporation of the solvent at rotary evaporator and finally dried in vacuo, using a vacuum desiccator for approximately 24 h. Yield 0.289 g (75%). ^{1}H NMR (300 MHz, CD_3OD, δ/ppm, *J*/Hz): 7.12 (1H, s) 6.74 (1H, s) 3.91 (3H, s) 3.89 (3H, s) 3.57 (3H, s) 2.02 (3H, s); HRMS-ESI (*m/z*): $[M+Na]^+$ calcd for $C_{21}H_{24}N_2O_5Na$: 407.1577, found: 407.1837.

General procedure for the synthesis of colchicine-amino acid derivatives (14a–d): To a solution of colchicine (80/160 mg) in 0.5 mL of 96% EtOH, the 10-fold molar equivalent of the appropriate

amino acid, γ-aminobutyric acid (for **15b**, **16**), (*S*)-(−)-4-amino-2-hydroxybutyric acid (for **17b**, **18**), ε-aminocaproic acid (for **19b**), 8-aminooctanoic acid (for **20b**) and 0.6 mL 1 M NaOH in 1.55 mL distilled H_2O were added. The resulting mixture was then stirred for 24 h at 1000 rpm. The end of the occurring reaction was confirmed by TLC. As a next step, the mixture was acidulated with 1 M HCl until it reached pH 5–6 depending on the acid used. Then the organic solvent was carefully removed in vacuo in a rotary evaporator and the aqueous layer was extracted with 3×15 mL EtOAc. The obtained extract was then dried over $MgSO_4$, filtered and resulting solution checked by TLC again. In the following, the compound was purified by flash column chromatography with evaporation of the solvent at rotary evaporator and finally dried in vacuo, using a vacuum desiccator for approximately 24 h.

14a Yield 0.140 g (74%). ^{1}H NMR (300 MHz, CD_3OD δ/ppm, *J*/Hz): 7.40 (d, *J* = 11.4 Hz, 1H), 7.25 (s, 1H), 6.82 (d, *J* = 11.4 Hz, 1H), 6.67 (s, 1H), 4.47 (dd, *J* = 12.0, 6.2 Hz, 1H), 3.85 (s, 3H, OCH_3), 3.84 (s, 3H, OCH_3), 3.52 (s, 3H, OCH_3), 3.42 (t, *J* = 7.0 Hz, 2H), 2.35 (t, *J* = 7.0 Hz, 2H), 2.07–2.30 (m, 2H), 1.99 ppm (s, 3H, NAc); HRMS-ESI (*m/z*): $[M+H]^+$ calcd for $C_{25}H_{30}N_2O_7$: 471.2126, found: 471.2442; $[M+Na]^+$ calcd for $C_{25}H_{30}N_2O_7Na$: 493.1945, found: 493.2273.

14b Yield 0.149 g (77%). ^{1}H NMR (300 MHz, CD_3OD δ/ppm, *J*/Hz): 7.38 (d, *J* = 11.4 Hz, 1H), 7.27 (s, 1H), 6.82 (d, *J* = 11.6 Hz, 1H), 6.68 (s, 1H), 4.49 (dd, *J* = 11.9, 6.1 Hz, 1H), 3.87 (s, 3H, OCH_3), 3.86 (s, 3H, OCH_3), 3.53 (s, 3H, OCH_3), 2.48–2.58 (m, 1H), 2.11–2.32 (m, 3H), 1.99 ppm (s, 3H, NAc); HRMS-ESI (*m/z*): $[M+Na]^+$ calcd for $C_{25}H_{30}N_2O_8Na$: 509.1894, found: 509.1898.

14c Yield 0.032 g (52%). ^{1}H NMR (300 MHz, $CDCl_3$ δ/ppm, *J*/Hz): δ = 7.51 (s, 1H), 7.44 (d, *J* = 11.3 Hz, 1H), 6.63 (d, *J* = 11.4 Hz, 1H), 6.52 (s, 1H), 4.67 (dd, *J* = 11.8, 5.9 Hz, 1H), 3.91 (s, 3H), 3.87 (s, 3H), 3.58 (s, 3H), 2.40–2.51 (m, 1H), 2.15–2.38 (m, 4H), 1.97 (s, 3H), 1.62–1.83 (m, 5H), 1.43–1.55 ppm (m, 2H); HRMS-ESI (*m/z*): $[M+Na]^+$ calcd for $C_{27}H_{33}N_2O_7Na$: 521.2264, found: 521.2232.

14d Yield 0.151 g (96%). ^{1}H NMR (300 MHz, CD_3OD δ/ppm, *J*/Hz): 7.43 (d, *J* = 11.4 Hz, 1H), 7.26 (s, 1H), 6.82 (d, *J* = 11.4 Hz, 1H), 6.70 (s, 1H), 4.49 (dd, *J* = 12.1, 6.2 Hz, 1H), 3.88 (s, 3H, OCH_3), 3.87 (s, 3H, OCH_3), 3.54 (s, 3H, OCH_3), 1.99 (s, 3H, NAc), 1.74 (quin, *J* = 7.1 Hz, 2H), 1.61 (quin, *J* = 7.2 Hz, 2H), 1.31–1.50 ppm (m, 8H); HRMS-ESI (*m/z*): $[M+Na]^+$ calcd for $C_{29}H_{38}N_2O_7Na$: 549.2571, found: 549.2639.

General procedure for the synthesis of compounds 15b, 16, 17b, 18, 19b, 20b by coupling hCE1-sensitive motifs with a C_{10}-demethoxyolchicine amino acid derivative: The carboxylic acid (**14a–d**) was dissolved in 3 mL of dry DMF by stirring at RT. A double, respectively threefold molar equivalent of DIPEA was added by syringe and stirred 10 min. Then a double molar equivalent of HATU was added as a solid and the resulting clear solution was stirred for 10 min at RT. The appropriate hCE1-sensitive motif (1,2) was added in a surplus (up to fivefold molar equivalent) and the resulting solution was stirred 24 h. Completion of the reaction was monitored by TLC. Then the solution was diluted with H_2O and extracted with 3×15 mL EtOAc. The received extract was then dried over $MgSO_4$, filtered and the resulting solution was checked by TLC again. In the following, the compound was purified by flash column chromatography and finally dried in vacuo, using a vacuum desiccator for approximately 24 h.

15b Yield 0.015 g (38%). ^{1}H NMR (300 MHz, CD_3OD δ/ppm, *J*/Hz): 7.97 (s, 1H), 7.44 (d, *J* = 11.3 Hz, 1H), 7.26 (s, 1H), 6.87 (d, *J* = 11.4 Hz, 1H), 6.71 (s, 1H), 4.50 (dd, *J* = 12.2, 6.2 Hz, 1H), 4.32–4.39 (m, 1H), 3.88 (s, 3H, OCH_3), 3.86 (s, 3H, OCH_3), 3.54 (s, 3H, OCH_3), 2.01–2.49 (m, 6H), 1.99 (s, 3H, NAc), 1.52–1.97 (m, 8H, cyclopentyl protons), 0.90 ppm (dd, *J* = 11.2, 6.4 Hz, 6H, $2CH_3$ leucine protons); HRMS-ESI (*m/z*): $[M+H]^+$ calcd for $C_{36}H_{49}N_3O_8$: 652.3592, found: 652.3696; $[M+Na]^+$ calcd for $C_{36}H_{49}N_3O_8Na$: 674.3412, found: 674.3520.

16 Yield 0.015 g (37%). ^{1}H NMR (300 MHz, CD_3OD δ/ppm, *J*/Hz): 7.97 (s, 1H), 7.46–7.30 (m, 5H, phenylglycine aromatic protons), 6.85 (dd, *J* = 11.4, 2.3 Hz, 1H), 6.71 (s, 1H), 5.39 (s, 1H), 3.88 (s, 3H, OCH_3), 3.86 (s, 3H, OCH_3), 3.53 (s, 3H, OCH_3), 2.02–2.47 (m, 6H), 1.98 (s, 3H, NAc), 1.43–1.78 ppm (m, 8H, cyclopentyl protons); HRMS-ESI (*m/z*): $[M+H]^+$ calcd for $C_{38}H_{45}N_3O_8$: 672.3279, found: 672.3339; $[M+Na]^+$ calcd for $C_{38}H_{45}N_3O_8Na$: 694.3099, found: 694.3167.

17b Yield 0.013 g (28%).^{1}H NMR (300 MHz, CD_3OD δ/ppm, *J*/Hz): 7.48 (d, *J* = 11.3 Hz, 1H), 7.29 (s, 1H), 6.87 (d, *J* = 11.3 Hz, 1H), 6.74 (s, 1H), 3.92 (s, 3H, OCH_3), 3.90 (s, 3H, OCH_3), 3.57 (s, 3H, OCH_3), 3.02 (d, *J* = 0.3 Hz, 1H), 2.88 (d, *J* = 0.7 Hz, 1H), 2.55–2.65 (m, 1H), 2.21 (br s, 4H), 2.02 (s, 3H, NAc), 1.48–1.92 (m, 8H), 0.88 ppm (dd, *J* = 11.2, 6.3 Hz, 6H, $2CH_3$ leucine protons); HRMS-ESI (*m/z*): $[M+H]^+$ calcd for $C_{36}H_{49}N_3O_9$: 668.3542, found: 668.3609; $[M+Na]^+$ calcd for $C_{36}H_{49}N_3O_9Na$: 690.3361, found: 690.3427.

18 Yield 0.012 g (25%).^{1}H NMR (300 MHz, CD_3OD δ/ppm, *J*/Hz): 7.28–7.41 (m, 5H, phenylglycine aromatic protons), 6.89 (d, *J* = 11.4 Hz, 1H), 6.74 (s, 1H), 3.92 (s, 3H, OCH_3), 3.90 (s, 3H, OCH_3), 3.57 (s, 3H, OCH_3), 3.02 (d, *J* = 0.3 Hz, 1H), 2.05 (s, 3H, NAc), 2.02 (s, 3H), 1.42–1.95 ppm (m, 8H, cyclopentyl protons); HRMS-ESI (*m/z*): $[M+H]^+$ calcd for $C_{38}H_{45}N_3O_9$: 688.3229, found: 688.3282; $[M+Na]^+$ calcd for $C_{38}H_{45}N_3O_9Na$: 710.3048, found: 710.3125.

19b Yield 0.066 g (91%). ^{1}H NMR (300 MHz, $CDCl_3$ δ/ppm, *J*/Hz): δ = 6.60 (d, *J* = 11.4 Hz, 1H), 6.54 (s, 1H), 6.10 (d, *J* = 8.1 Hz, 1H), 3.94 (s, 3H, OCH_3), 3.90 (s, 3H, OCH_3), 3.62 (s, 3H, OCH_3), 2.00 (s, 3H, NAc), 1.44–1.96 (m, 18H, cyclopentyl and caproic acid protons), 0.94 ppm (*J* = 11.1, 6.4 Hz, 6H, CH_3 leucine protons); HRMS-ESI (*m/z*): $[M+Na]^+$ calcd for $C_{38}H_{53}N_3O_8Na$: 702.3730, found: 702.3807.

20b Yield 0.040 g (94%). ^{1}H NMR (300 MHz, CD_3OD δ/ppm, *J*/Hz): 7.47 (d, *J* = 11.3 Hz, 2H), 7.28 (s, 1H), 6.85 (d, *J* = 11.4 Hz, 2H), 6.73 (s, 2H), 3.91 (s, 3H, OCH_3), 3.90 (s, 3H, OCH_3), 3.57 (s, 3H, OCH_3), 2.01 (s, 3H, NAc), 1.54–1.92 (m, 8H, cyclopentyl protons), 1.33–1.53 (m, 8H, octanoic acid protons), 0.92 ppm (*J* = 11.1, 6.4 Hz, 6H, $2CH_3$ leucine protons); HRMS-ESI (*m/z*): $[M+Na]^+$ calcd for $C_{40}H_{57}N_3O_8Na$: 730.4038, found: 730.4071.

Synthesis of 21b: First, to a solution of 4-carboxybenzylaldehyde (348 mg, 2.25 mmol) in THF (25 mL) was added tosylate salt of cyclopentyl L-leucinate (**5**) (890 mg, 2.25 mmol) or chloride of cyclopentyl L-phenylgycinate (**6**) (0.581 mg, 2.25 mmol), stirred for 60 min, and then portion-wise sodium triacetoxyborohydride (1192 mg, 4.5 mmol). The mixture was stirred for 18 h at RT. Then it was diluted with EtOAc and dried over $MgSO_4$, filtered and the resulting solution was checked by TLC again. In the following, the compound was purified by flash column chromatography and finally dried in vacuo, using a vacuum desiccator for approximately 24 h. 99 mg (0.3 mmol) of the obtained cyclopentyl *N*-(4-carboxybenzyl)-L-leucinate or 105 mg of cyclopentyl *N*-(4-carboxybenzyl)-L-phenylglycinate dissolved in 2 mL CH_2Cl_2 and added several drops DMF. Then 22 μL $SOCl_2$ were added and the mixture was held at reflux for 1 h. After this, the solution of 0.058 g **13** in 1 mL of pyridine was added and the mixture was stirred at RT for 2 h more. The organic solvent was washed with H_2O and evaporated under reduced pressure and the aqueous phase extracted three times with 5 mL EtOAc. The extract was dried over $MgSO_4$, filtered and

the resulting solution checked by TLC again. In the following, the compound was purified by flash column chromatography and finally dried in vacuo, using a vacuum desiccator for approximately 24 h.

21 b Yield 0.050 g (48%). ^{1}H NMR (300 MHz, $CDCl_3$ δ/ppm, *J*/Hz): 7.87–8.15 (m, 4H), 7.62–7.69 (m, 2H, aromatic protons), 7.46–7.59 (m, 2H, aromatic protons), 6.53–6.56 (m, 1H), 3.97 (s, 3H, OCH_3), 3.94 (s, 3H), 3.66 (s, 3H, OCH_3), 2.09 (s, 3H, NAc), 1.56–1.94 (m, 13H), 0.91 ppm (dd, $J=17.1$, 6.5 Hz, 6H, $2CH_3$ leucine protons); HRMS-ESI (*m/z*): $[M+H]^+$ calcd for $C_{40}H_{49}N_3O_8$: 700.3592, found: 700.3835; $[M+Na]^+$ calcd for $C_{40}H_{49}N_3O_8Na$: 722.3412 found: 722.3659.

General procedure for the synthesis of metabolites (15 a, 17 a, 19 a, 20 a, 21 a): The metabolites of the studied compounds were synthesized according to the procedures provided above, but replacing the cyclopentyl esters of Leu and Phg with *tert*-butyl esters of the same amino acids. The obtained *tert*-butyl derivatives were subjected to hydrolysis with aqueous phosphoric acid as follows: 0.045 mmol of the respective *tert*-butyl ester were dissolved in 3 mL CH_2Cl_2 and 0.116 mL of 85% aqueous phosphoric acid were added dropwise at room temperature. The mixture was vigorously stirred for 3 h and the reaction checked by HPLC. Then 5 mL of H_2O was added and the mixture was cooled to 0 °C. A saturated solution of $NaHCO_3$ was added slowly to adjust the pH to 8. The mixture was then extracted with EtOAc. The combined organic phase was dried over magnesium sulfate and concentrated in vacuo to obtain the product.

15 a HRMS-ESI (*m/z*): $[M-H]^-$ calcd for $C_{31}H_{41}N_3O_8$: 582.2821, found: 582.2821.

17 a ^{1}H NMR (300 MHz, CD_3OD δ/ppm, *J*/Hz): 7.44 (d, $J=11.3$ Hz, 1H), 7.26 (s, 1H), 6.82 (d, $J=11.4$ Hz, 1H), 6.71 (s, 1H), 3.88 (s, 3H, OCH_3), 3.87 (s, 3H, OCH_3), 3.55 (s, 3H, OCH_3), 1.99 (s, 3H, NAc), 1.51–1.66 (m, 3H), 0.85 ppm (dd, $J=11.7$, 6.3 Hz, 6H, $2CH_3$ leucine protons); HRMS-ESI (*m/z*): $[M-H]^-$ calcd for $C_{35}H_{41}N_3O_8$: 630.2821, found: 630.2729.

19 a ^{1}H NMR (300 MHz, CD_3OD δ/ppm, *J*/Hz): 7.44 (d, $J=11.3$ Hz, 1H), 7.27 (s, 1H), 6.83 (d, $J=11.4$ Hz, 1H), 6.70 (s, 1H), 3.88 (s, 3H, OCH_3), 3.87 (s, 3H, OCH_3), 3.54 (s, 3H, OCH_3), 1.99 (s, 3H, NAc), 0.91 ppm (dd, $J=6.2$, 1.2 Hz, 6H, $2CH_3$ leucine protons); HRMS-ESI (*m/z*): $[M-H]^-$ calcd for $C_{33}H_{45}N_3O_8$: 610.3134, found: 610.3158.

20 a HRMS-ESI (*m/z*): $[M-H]^-$ calcd for $C_{35}H_{49}N_3O_8$: 638.3447, found: 638.3443.

21 a ^{1}H NMR (300 MHz, CD_3OD δ/ppm, *J*/Hz): 7.97–8.04 (m, $J=$ 8.4 Hz, 2H, aromatic protons), 7.62–7.69 (m, $J=8.4$ Hz, 2H, aromatic protons), 7.52 (s, 1H), 7.48 (d, $J=10.8$ Hz, 1H), 6.75 (s, 1H), 3.90 (s, 3H, OCH_3), 3.89 (s, 3H, OCH_3), 3.61 (s, 3H, OCH_3), 2.00 ppm (s, 3H, NAc), 0.94 ppm (dd, $J=6.2$, 1.2 Hz, 6H, $2CH_3$ leucine protons); HRMS-ESI (*m/z*): $[M-H]^-$ calcd for $C_{31}H_{41}N_3O_9$: 598.2770, found: 598.2762.

Expression and purification of the human carboxylesterase 1: Human carboxylesterase was expressed in Sf9 insect cells using the baculovirus expression system. In brief, the coding sequence of hCE1 was amplified from cDNA of HeLa cells and cloned into pFASTBac1 vector by a PCR-based cloning approach using the primer pair RF_hCE_FW (CACCATCGGGCGCGGATATGTGGCTCCGTGCCT) and RF_hCE_REV (GCTGATTATGATCCTCTAGTACTTCTCGACAAGCTAGTGATGGTGATGGTGATGCAGCTCTATGTGTTCTGTCTGG). *E. coli* DH10Bac cells were transformed with the resulting plasmid, pFastBac1-hCE1, in order to generate recombinant bacmid. The extracted recombinant bacmid DNA was transfected into Sf9 cells using Cellfectin transfection reagent (Thermo Fisher Scientific) according to the supplier's instruction manual in order to generate recombinant baculoviruses. After 72 h, supernatant was harvested and viral titer was determined by plaque assay. For expression of hCE1, Sf9 cells were infected with recombinant baculovirus with a multiplicity of infection (MOI) of 10 and incubated for 72 h at 27 °C. After harvesting the cells by centrifugation at $1000\times g$ for 15 min, cells were lysed by adding lysis buffer (50 mM HEPES, pH 7.5, 150 mM NaCl, 5 mM 2-mercaptoethanol, 0.05% Triton X-100) and sonication. Insoluble components were separated by centrifugation at 4 °C at $45\,000\times g$ for 45 min. The hCE1 protein was subsequently purified by Ni-affinity chromatography and size exclusion chromatography.

Virus titer reduction assay (plaque assay): Huh7 and Vero E6 cells were maintained in Dulbecco's modified Eagle's medium (DMEM) supplemented with 10% fetal bovine serum, penicillin G (100 U mL^{-1}) and 0.1 mg mL^{-1} streptomycin (DMEMcplt) at 37 °C, 5% CO_2, and 95% relative humidity. For assessing cytotoxicity, 10^4 Huh7 cells per well were seeded into 96-well plates in 50 μL DMEMcplt and incubated overnight at 37 °C. On the next day, the cells were infected with wild-type DENV serotype 2 with a multiplicity of infection (MOI) of 1 in the presence of the respective concentration of the tested compound in triplicates. After incubation for 48 h at 37 °C the medium was harvested, the triplicates were pooled and stored at −80 °C until further use. 50 μL of fresh DMEMcplt was added to the cells and cell viability was determined using Cell-Titer Glo Luminescent Viability Assay (Promega). For measurement of virus titers by plaque assay, Vero E6 cells were seeded into 24-well plates at a density of 2.5×10^5 cells per well. After overnight incubation at 37 °C, the cells were inoculated with the harvested virus supernatant that was diluted with DMEMcplt ranging from 10^{-1} to 10^{-6} prior to inoculation. After incubation of the cells with 100 μL of the virus dilution at 37 °C with agitation for 1 h, the medium was removed and 1 mL of plaque medium was added. After further incubation for 7 days at 37 °C the cells were fixed with 5% (*v/v*) formaldehyde for 2 h, stained with crystal violet and plaques were counted. Titer reduction was calculated relative to a control treated with DMSO alone.

Toxicity assay: Determination of cell viability was performed using the Cell Titer Blue assay with HeLa or Huh7 cells. All tested compounds were diluted in a dilution series from 50 μM down to 3.2 nM in a sterile flat-bottom 96-well plate with a zero compound control. HeLa and Huh7 cells were cultivated in DMEM. After splitting, the cells were diluted with DMEM and 5000 HeLa cells or 7000 Huh7 cells were put into each well of the initial plate and incubated for 24 and 72 h at 37 °C. After the incubation, the medium was removed with a vacuum pump and 100 μL of a mixture of 20% resazurin and 80% DMEM was aliquoted into the wells. The dye was incubated for 2 h at 37 °C. Afterward, the percentage of cell viability was calculated by the difference of absorption at 570 nm and 600 nm. CC_{50} values were obtained after plotting cell viability versus the logarithmic concentration and applying a dose–response fit in GraphPad Prism 7.

Hydrolysis of compounds by hCE1: The biochemical assay was performed in a 96-well U-bottom plate. In assay buffer (20 mM phosphate pH 7.4 with 40 mM KCl), a 10 mM compound stock solution in DMSO was diluted to 10 μM. hCE1 solution was added to a final concentration of 100 nM. The plate was incubated at 37 °C for 2 h. Subsequently, the assay was quenched with the addition of 30 μL acetonitrile per well. The relative concentration of the compound was then determined by integration of HPLC signals and

compared with a control without enzyme. In cases where no cleavage was observed in 2 h, the compounds were incubated for 24 h in order to confirm the lack of cleavage.

Tubulin polymerization assay: The assay was performed in a 96-well flat-bottom plate using a porcine tubulin polymerization assay kit by tebu-bio GmbH (Germany). To prepare the 5 mg mL^{-1} stock solution of tubulin 4 mg of lyophilized tubulin was dissolved in 800 μL of cold "general tubulin buffer" (GTB, 80 mM PIPES, 0.5 mM EGTA, 2 mM $MgCl_2$, pH 6.9). 100 μM stock solutions of the analyzed compounds were prepared by diluting 0.1 mL of the 10 mM DMSO-based solution of the compound in 9.9 mL GTB. In each analytical well 80 μL of tubulin solution in GTB, 10 μL 10× compound solution in GTB, 10 μL GTP solution in GTB were added reaching the respective final concentrations of 4 mg mL^{-1} tubulin, 10 μM compound, and 1 mM GTP. In each control well 80 μL of tubulin solution in GTB, 10 μL of DMSO in GTB (0.1 mL in 9.9 mL), and 10 μL GTP in GTB were added to yield final concentrations of 4 mg mL^{-1} for tubulin and 1 mM for GTP. *Procedure*: The plate was incubated at 37 °C for 30 min with added solutions of tubulin and the test compound, followed by chilling to 0 °C to depolymerize formed microtubules. Subsequently, GTP solution was added. Immediately after the addition of GTP, the read-out began. For read-out, the absorption at 340 nm and 37 °C was measured by a microtiter plate reader (BMG labtech Omega).

Molecular modelling studies: Docking simulation study was performed using Molecular Operating Environment (MOE), Chemical Computing Group Inc., (2015), 1010 Sherbrooke St. West, Suite #910, Montreal, QC, H3A 2R7 (Canada). The computational software operated under Windows 8 Pro (64 bit) installed on a Dell Precision T7610 (v3) workstation. The X-ray crystallographic structure of tubulin in complex with colchicine was obtained from the RCSB Protein Data Bank (PDB, http://www.rcsb.org/, PDB ID: 4OB2).[57] The corresponding structure of combretastatin was also obtained from the PDB, PDB ID: 1LYJ.[24] The energy of all conformers was minimized in an automatic mode until the RMSD gradient of 0.01 kcal mol^{-1} was achieved, and the mean square distance of 0.1 Å was calculated with the force field MMFF94X.

Acknowledgements

*V.B. is grateful for generous funding under the Georg Forster Research Fellowship received from the Alexander von Humboldt Foundation. The authors acknowledge the technical assistance of Stephanie Kallis for the ZIKV antiviral assay, Natascha Stefan for the help in cell culture, and Heiko Rudy for the mass spectrometry data. M.R. thanks Torben LangHeinrich for his assistance in the synthesis of compound **9a**.*

Conflict of interest

The authors declare no conflict of interest.

Keywords: antiviral agents · colchicine · combretastatin · dengue · prodrugs · tubulin ligands · Zika

[1] S. Bhatt, P. W. Gething, O. J. Brady, J. P. Messina, A. W. Farlow, C. L. Moyes, J. M. Drake, J. S. Brownstein, A. G. Hoen, O. Sankoh, M. F. Myers, D. B. George, T. Jaenisch, G. R. Wint, C. P. Simmons, T. W. Scott, J. J. Farrar, S. I. Hay, *Nature* **2013**, *496*, 504 – 507.

[2] J. D. Stanaway, D. S. Shepard, E. A. Undurraga, Y. A. Halasa, L. E. Coffeng, O. J. Brady, S. I. Hay, N. Bedi, I. M. Bensenor, C. A. Castañeda-Orjuela, T.-W. Chuang, K. B. Gibney, Z. A. Memish, A. Rafay, K. N. Ukwaja, N. Yonemoto, C. J. L. Murray, *Lancet Infect. Dis.* **2016**, *16*, 712 – 723.

[3] S. C. Weaver, W. K. Reisen, *Antiviral Res.* **2010**, *85*, 328 – 345.

[4] V. Boldescu, M. A. M. Behnam, N. Vasilakis, C. D. Klein, *Nat. Rev. Drug Discovery* **2017**, *16*, 565 – 586.

[5] S. H. E. Kaufmann, A. Dorhoi, R. S. Hotchkiss, R. Bartenschlager, *Nat. Rev. Drug Discovery* **2017**, *17*, 35 – 56.

[6] W. MacRae, J. Hudson, G. Towers, *Planta Med.* **1989**, *55*, 531 – 535.

[7] M. Cortese, S. Goellner, E. G. Acosta, C. J. Neufeldt, O. Oleksiuk, M. Lampe, U. Haselmann, C. Funaya, N. Schieber, P. Ronchi, M. Schorb, P. Pruunsild, Y. Schwab, L. Chatel-Chaix, A. Ruggieri, R. Bartenschlager, *Cell Rep.* **2017**, *18*, 2113 – 2123.

[8] M. Satake, R. B. Luftig, *J. Gen. Virol.* **1982**, *58*, 339 – 349.

[9] K. Y. Foo, H. Chee, *Biomed Res. Int.* **2015**, *2015*, 1 – 6.

[10] E. G. Acosta, V. Castilla, E. B. Damonte, *J. Gen. Virol.* **2008**, *89*, 474 – 484.

[11] M. S. Paingankar, M. D. Gokhale, D. N. Deobagkar, *Arch. Virol.* **2010**, *155*, 1453 – 1461.

[12] W. Chen, N. Gao, J. L. Wang, Y. P. Tian, Z. T. Chen, J. An, *Arch. Virol.* **2008**, *153*, 1777 – 1781.

[13] U. F. Greber, *Cell. Mol. Life Sci.* **2002**, *59*, 608 – 626.

[14] R. Thayan, T. L. Huat, L. L. C. See, N. S. Khairullah, R. Yusof, S. Devi, *Southeast Asian J. Trop. Med. Public Health* **2009**, *40*, 56 – 65.

[15] E. G. Acosta, V. Castilla, E. B. Damonte, *Cell. Microbiol.* **2009**, *11*, 1533 – 1549.

[16] H. Y. Chee, S. AbuBakar, *Biochem. Biophys. Res. Commun.* **2004**, *320*, 11 – 17.

[17] B. E. E. Martina, P. Koraka, A. D. M. E. Osterhaus, *Clin. Microbiol. Rev.* **2009**, *22*, 564 – 581.

[18] S. Blackley, Z. Kou, H. Chen, M. Quinn, R. C. Rose, J. J. Schlesinger, M. Coppage, X. Jin, *J. Virol.* **2007**, *81*, 13325 – 13334.

[19] V. Boldescu, V. Crudu, N. Sucman, S. Pogrebnoi, M. Zviaghin, E. Stîngaci, V. Pogrebnoi, F. Macaev, *Chem. J. Mold.* **2013**, *8*, 21 – 31.

[20] M. Hosokawa, *Molecules* **2008**, *13*, 412 – 431.

[21] L. A Needham, A. H. Davidson, L. J. Bawden, A. Belfield, E. A. Bone, D. H. Brotherton, S. Bryant, M. H. Charlton, V. L. Clark, S. J. Davies, A. Donald, F. A. Day, D. Krige, V. Legris, J. McDermott, Y. McGovern, J. Owen, S. R. Patel, S. Pintat, R. J. Testar, G. M. Wells, D. Moffat, A. H. Drummond, *J. Pharmacol. Exp. Ther.* **2011**, *339*, 132 – 142.

[22] M. H. Charlton, D. F. C. Moffat, S. J. Davies, A. H. Drummond (Chroma Therapeutics Ltd.), US Pat. No. US20140010762 A1, **2014**.

[23] R. B. G. Ravelli, B. Gigant, P. A. Curmi, I. Jourdain, S. Lachkar, A. Sobel, M. Knossow, *Nature* **2004**, *428*, 198 – 202.

[24] R. Gaspari, A. E. Prota, K. Bargsten, A. Cavalli, M. O. Steinmetz, *Chem* **2017**, *2*, 102 – 113.

[25] J. A. Woods, J. A. Hadfield, G. R. Pettit, B. W. Fox, A. T. McGown, *Br. J. Cancer* **1995**, *71*, 705 – 711.

[26] K. Jaroch, M. Karolak, P. Górski, A. Jaroch, A. Krajewski, A. Ilnicka, A. Sloderbach, T. Stefański, S. Sobiak, *Pharmacol. Rep.* **2016**, *68*, 1266 – 1275.

[27] M. Medarde, A. B. S. Maya, C. Pérez-Melero, *J. Enzyme Inhib. Med. Chem.* **2004**, *19*, 521 – 540.

[28] R. Mikstacka, T. Stefański, J. Różański, *Cell. Mol. Biol. Lett.* **2013**, *18*, 368 – 397.

[29] G. C. Tron, T. Pirali, G. Sorba, F. Pagliai, S. Busacca, A. A. Genazzani, *J. Med. Chem.* **2006**, *49*, 3033 – 3044.

[30] C. Da, S. L. Mooberry, J. T. Gupton, G. E. Kellogg, *J. Med. Chem.* **2013**, *56*, 7382 – 7395.

[31] A. Vandecandelaere, S. R. Martin, P. M. Bayley, M. J. Schilstra, *Biochemistry* **1994**, *33*, 2792 – 2801.

[32] B. Baguley, L. Zhuang, P. Kestell, *Oncol. Res.* **1997**, *9*, 55 – 60.

[33] J. Fournier-Dit-Chabert, V. Vinader, A. R. Santos, M. Redondo-Horcajo, A. Dreneau, R. Basak, L. Cosentino, G. Marston, H. Abdel-Rahman, P. M. Loadman, *Bioorg. Med. Chem. Lett.* **2012**, *22*, 7693 – 7696.

[34] M. Roesner, H.-G. Capraro, A. E. Jacobson, L. Atwell, A. Brossi, M. A. Iorio, T. H. Williams, R. H. Sik, C. F. Chignell, *J. Med. Chem.* **1981**, *24*, 257 – 261.

[35] A. Huczyński, J. Rutkowski, K. Popiel, E. Maj, J. Wietrzyk, J. Stefańska, U. Majcher, F. Bartl, *Eur. J. Med. Chem.* **2014**, *90*, 296 – 301.

[36] Y. B. Malysheva, S. Combes, D. Allegro, V. Peyrot, P. Knochel, A. E. Gavryushin, A. Y. Fedorov, *Bioorg. Med. Chem.* **2012**, *20*, 4271 – 4278.

[37] N. Yasobu, M. Kitajima, N. Kogure, Y. Shishido, T. Matsuzaki, M. Nagaoka, H. Takayama, *ACS Med. Chem. Lett.* **2011**, *2*, 348 – 352.
[38] E. O. Esbolaev, N. A. Aitkhozhina, L. A. Aleksandrova, *Chem. Nat. Compd.* **1989**, *25*, 80 – 83.
[39] Y. L. Garazd, M. M. Garazd, V. G. Kartsev, *Chem. Nat. Compd.* **2015**, *51*, 1138 – 1141.
[40] A. Massarotti, A. Coluccia, R. Silvestri, G. Sorba, A. Brancale, *ChemMedChem* **2012**, *7*, 33 – 42.
[41] A. Farce, C. Loge, S. Gallet, N. Lebegue, P. Carato, P. Chavatte, P. Berthelot, D. Lesieur, *J. Enzyme Inhib. Med. Chem.* **2004**, *19*, 541 – 547.
[42] O. M. Aly, E. A. Beshr, R. M. Maklad, M. Mustafa, A. M. Gamal-Eldeen, *Arch. Pharm.* **2014**, *347*, 658 – 667.
[43] M. Mphahlele, N. Parbhoo, *Pharmaceuticals* **2018**, *11*, 59.
[44] M. Zayed, S. Ahmed, S. Ihmaid, H. Ahmed, H. Rateb, S. Ibrahim, *Int. J. Mol. Sci.* **2018**, *19*, 1731.
[45] S. N. Baytas, N. Inceler, A. Yılmaz, A. Olgac, S. Menevse, E. Banoglu, E. Hamel, R. Bortolozzi, G. Viola, *Bioorg. Med. Chem.* **2014**, *22*, 3096 – 3104.
[46] M.-M. Niu, J. Qin, C. Tian, X. Yan, F.-G. Dong, Z. Cheng, G. Fida, M. Yang, H. Chen, Y. Gu, *Acta Pharmacol. Sin.* **2014**, *35*, 967 – 979.
[47] U. Yadava, V. K. Yadav, R. K. Yadav, *RSC Adv.* **2017**, *7*, 15917 – 15925.
[48] Y. Wang, H. Zhang, B. Gigant, Y. Yu, Y. Wu, X. Chen, Q. Lai, Z. Yang, Q. Chen, J. Yang, *FEBS J.* **2016**, *283*, 102 – 111.
[49] B. V. Kumbhar, A. Borogaon, D. Panda, A. Kunwar, *PLoS One* **2016**, *11*, e0156048.
[50] R. I. Ahmed, E. E. A. Osman, F. M. Awadallah, S. M. El-Moghazy, *J. Enzyme Inhib. Med. Chem.* **2017**, *32*, 176 – 188.
[51] D. D. Li, Y. J. Qin, X. Zhang, Y. Yin, H. L. Zhu, L. G. Zhao, *Chem. Biol. Drug Des.* **2015**, *86*, 731 – 745.
[52] D. F. Tang-Wai, P. Gros, A. Brossi, L. D. Arnold, *Biochemistry* **1993**, *32*, 6470 – 6476.
[53] S. Bencharit, C. C. Edwards, C. L. Morton, E. L. Howard-Williams, P. Kuhn, P. M. Potter, M. R. Redinbo, *J. Mol. Biol.* **2006**, *363*, 201 – 214.
[54] T. Fukami, M. Kariya, T. Kurokawa, A. Iida, M. Nakajima, *Eur. J. Pharm. Sci.* **2015**, *78*, 47 – 53.
[55] S. Casey Laizure, V. Herring, Z. Hu, K. Witbrodt, R. B. Parker, *Pharmacother. J. Hum. Pharmacol. Drug Ther.* **2013**, *33*, 210 – 222.
[56] C. Liang, M. A. M. Behnam, T. R. Sundermann, C. D. Klein, *Tetrahedron Lett.* **2017**, *58*, 2325 – 2329.
[57] A. E. Prota, F. Danel, F. Bachmann, K. Bargsten, R. M. Buey, J. Pohlmann, S. Reinelt, H. Lane, M. O. Steinmetz, *J. Mol. Biol.* **2014**, *426*, 1848 – 1860.

Manuscript received: September 28, 2018
Revised manuscript received: December 1, 2018
Accepted manuscript online: January 3, 2019
Version of record online: January 25, 2019